OPEN ACCESS

University of BRISTOL

Peer reviewed version

Link to published version (if available):
10.1109/TAP.2017.2748362

Link to publication record in Explore Bristol Research
PDF-document

University of Bristol - Explore Bristol Research
General rights

Off-Body Antenna Wireless Performance Evaluation in a Residential Environment

Sema Dumanli, Lawrence Sayer, Evangelos Mellios, Xenofon Fafoutis, *Member, IEEE,*
Geoffrey Hilton, Ian Craddock, *Fellow, IEEE*

Abstract—**Modern body-centric communication systems require good link quality. Antenna performance is of primary importance when meeting this requirement. This paper contributes a method suited to the difficult task of quantifying antenna performance in a body-centric communications system. In a case study, a planar wrist wearable antenna, which provides radiation pattern switching across the 2.4GHz operating band through an innovative technique that does not require an additional switching mechanism, is benchmarked against a monopole and a patch antenna in a residential setting. The performance of the antenna, and subsequently the benefits of the pattern switching technique, are successfully quantified. The holistic method includes both antenna measurements and channel simulation with ray-tracing. Results are verified against real world measurements.**

Index Terms—**Antenna radiation patterns, Bluetooth Low Energy, Body sensor networks, Microstrip antennas, Internet of Things, Indoor communication, Body-centric communications**

I. INTRODUCTION

The development of techniques to quantify antenna performance in body-centric communication systems is a pertinent problem given that recent advances in sensing technologies are a proposed solution to the challenges of modern healthcare [1]. Wearable sensing technologies [2] are valuable tools that can encourage people to monitor their own well-being and facilitate timely health interventions. Indeed, the rising popularity of commercial wearable gadgets, such as fitness trackers and smart watches, indicates a trend towards this direction. Yet, the utility of wearable sensors rises when they are used alongside other healthcare systems and sensing technologies within smart environments. In the upcoming era of Internet of Things (IoT), the future generation of wearable sensing devices will be required to communicate with different kinds of things in dynamic environments [3]. They must efficiently support not only on-body communications (such as between wearable sensors), but also off-body communications (such as wearable sensor to smart home) [4]. To support high quality data links these wearables must have good antenna performance.

Antennas and radio wave propagation constitute the basic elements of the wireless channel. They, therefore, determine the quality and the reliability of the wireless link and hence have a great impact on the Quality-of-Service (QoS) offered by a whole system. Modelling of both these aspects of the channel is of interest to device designers. In a body-centric wireless network, the human body imposes several extra challenges for propagation modelling and antenna testing, such as electromagnetic absorption, propagation shadowing and polarisation misalignment [5]-[9].

The off-body wireless performance of wearable antennas has thoroughly been investigated for Ultra-Wideband (UWB) communication systems that operate between 3.1 GHz and 10.6 GHz [10]-[13], and for applications in the 868 MHz frequency band [14], [15]. However, limited work has been published for applications in the 2.4 GHz band, in which the commonly used for low-power body-centric communications BLE technology operates. An experimental campaign presented in [16] and [17] investigates the off-body radio channel in the 2.4 GHz band in an anechoic chamber and in an office environment. Other off-body channel measurements at 2.4 GHz for specific applications and environments are presented in [18] (outdoors); in [19] and [20] (bed-side applications for sleep monitoring); in [21] (hospital environment); and in [22] (for hearing instrument applications). The IEEE 802.15.6 channel models [23] constitute a set of standardized models for in-body, on-body, body-to-body and off-body scenarios. The CM4 scenario refers to the off-body channel and is based on measurements conducted for a wrist and a chest worn antenna at 900 MHz, at 2.4 GHz, and at 3.1 to 10.6 GHz with a human body subject standing, walking and sleeping. Results include mean and variance of path-loss as a function of distance and body orientation for applications where the user and the access-point are in the same room.

This paper contributes a method by which the performance of a wearable antenna in a BLE in-home network can be quantified ensuring that high link quality is provided for body-centric applications. The method combines antenna characteristics with a physical model of the wireless channel and the communication system performance is evaluated for various antenna orientations and locations within a residential environment. In contrast, most methods in literature are constrained to either a particular room or specific link type. Physical modelling of the channel is performed using ray-tracing simulations. The ray-tracer provides the multipath propagation characteristics of the channel in a residential setting in which body-centric networks are likely to operate.

An on-body antenna design is then proposed and used as a candidate for evaluation of the proposed method. The antenna is a patch antenna which provides radiation pattern switching

S. Dumanli was with Toshiba Research Europe Ltd, Bristol, UK. She is now with Electrical and Electronics Engineering Department, Boğaziçi University, Istnabul, Turkey (semadumanli@gmail.com)
L. Sayer, E. Mellios, X. Fafoutis, G. Hilton, I. Craddock are with Electrical and Electronic Department, Bristol University, Bristol, UK (l.sayer, evangelos.mellios, xenofon.fafoutis, geoff.hilton ian.craddock@bristol.ac.uk)

across the 2.4 GHz operating band without an additional switching mechanism. This was achieved by merging an omnidirectional and a directional radiation mode of the antenna together within a single band, in contrast to the conventional procedure of covering the whole band with a single radiation mode. This proposal is a simple low-cost mechanism to improve connectivity significantly when the link is dynamic. Using the proposed method, the performance of this antenna is evaluated and its benefits are quantified over two conventional widely used antenna types with single radiation mode operation, a directional patch and an omnidirectional monopole.

To verify that our modelling gives accurate results the real world wireless performance of the proposed antenna is experimentally evaluated in a domestic environment. In the experiment, an on-body sensor node communicates with a nearby AP in the 2.4 GHz band using BLE.

II. PROPOSED METHOD

Human bodies are mobile which makes body centric networks dynamic. Since the design of an antenna will be constant, optimisations for performance where a person is in a particular room, in a particular pose, might negatively affect antenna performance where the person is somewhere else doing something else. This is why existing models are inappropriate for generating meaningful performance metrics. The antenna evaluation procedure we advocate in this paper is shown in Fig. 1. This is a holistic method for developing antenna designs which considers the antenna performance in a dynamic multipath environment rather than in isolation. Several different arrangements of the user and AP are tested, which gives a better indication of real world performance.
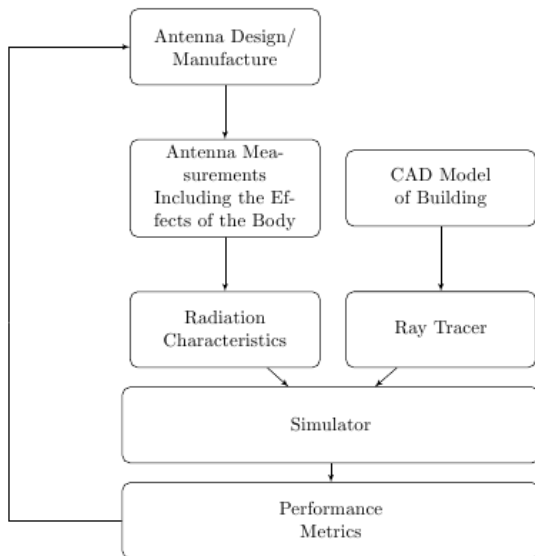

Fig. 1 An overview of the proposed method for antenna design and verification.

To produce a suitable antenna radiation model, accurate measurements of antenna pattern including the effects of the body are required. The antenna measurement campaign conducted for this paper includes anechoic chamber measurements of the antenna attached to a phantom in various positions. The use of rotating turntables allows a three-dimensional antenna pattern to be generated that includes the effects of being near the body. Computer scripts can be used to rotate an antenna pattern, with two polarisations, in 3D space to any required orientation.

The ray-tracer that we use includes reflections, refractions and diffraction of rays and has been verified against measurements in [24], [25], [26]. Rays represent the spherical travelling wave-front of the electromagnetic wave generated by a transmitter. Used at the frequencies of interest the ray-tracer can be considered state-of-the-art.

The ray-tracer takes as an input a computer aided design (CAD) model of the environment of interest. For the purposes of this paper, a model of a three-storey house on Woodland Road, Bristol, UK was used. This is shown in Fig. 2. The model includes both the spatial layout of the building, as well as material constitutive parameters. Client and access point locations are specified as needed. Complex phasors representing the signal in two orthogonal polarisations are traced through the environment, being modified as necessary by interactions with building materials and by propagation through space.
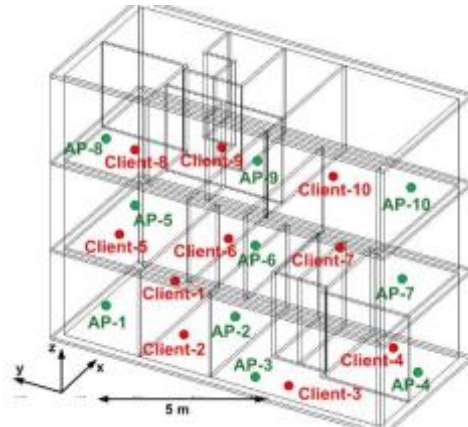

Fig. 2 Virtual 3D test-house showing all access-point and user (client) locations.

Analysing the time of arrival and state of phasors at the receive antenna allows for a power delay profile and other information, such as phase, polarisation and received signal strength to be derived. In ray-tracing all antennas are assumed to be isotropic and of unity gain. Using angle of arrival and departure information the radiation characteristics obtained from chamber measurements can be convolved with data generated from ray-tracing to simulate the whole channel.

We have taken care to ensure that inaccuracies introduced into the model, for example, due to unrepresentative material parameters, are kept to a minimum. Whilst there will inevitably be some inaccuracies there are several benefits to the use of ray tracing simulations. Results are more accurate/applicable than statistical models since more information about the environment is included. There is no requirement for engineers to disrupt a space or perform measurements, which might require expensive equipment. Data collection can also be automated and results can be generated in any environment where it is possible to generate a CAD model. Data visualisations such as ray paths can also be inspected to identify significant propagation routes or particularly problematic links.

III. On-body Antenna Example

A. Case study

The case study antenna design could be used to improve the performance of an off-body communication link in the home. This type of link might be used for sensing devices that need to communicate to infrastructure. The candidate antenna is a good example because it operates in a complex and dynamic environment in which measurements performed in a single room in a single orientation would be unrepresentative and where extensive measurements would be costly and time-consuming.

B. Antenna Design

Two different modes of a patch antenna have been merged within the 2.4 GHz ISM band. The dimensions of the antenna have been optimized in such a way that the two modes are adjacent to each other in the frequency domain. As the frequency of operation is changed, the radiation pattern can be steered. In a body-centric communication system that operates in the ISM band, interference rejection is typically realized with frequency hopping (e.g. BLE technology). With frequency hopping implemented at the link-layer, the transmitter and the receiver switch amongst multiple frequency channels, using a pre-agreed pseudo-random pattern. In this context, having a pool of channels with different radiation patterns can improve the robustness of the system [27]. This is going to be particularly helpful if the propagation channel is dynamic and the angle of arrival is changing quickly over the time.

The TM_{00} mode of a shorted rectangular patch antenna generates an omni-directional radiation pattern. It is comparable to the TM_{01} mode that appears in shorted ring patch antennas which has been widely studied in the literature [28]-[30] unlike the shorted rectangular patch. The omnidirectional mode in the shorted rectangular patch antennas having two symmetrical shorting pins was studied in [31] where it was referred to as a monopolar wire-patch antenna for frequencies situated below the fundamental cavity resonance mode. Its application to BAN was studied in [32] and the performance of the antenna was compared with a conventional patch and a monopole antenna near body surface and shown to be suitable for the application.
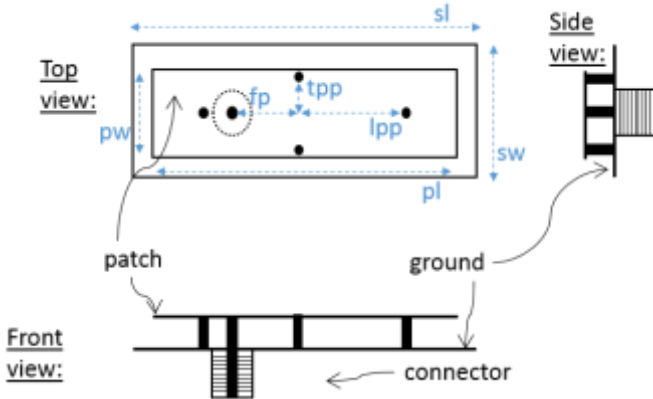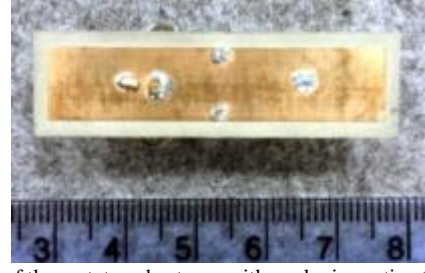

Fig. 4 Photo of the prototyped antenna with a ruler in centimetres.

Here the monopolar wire-patch antenna is designed with four shorting pins. The pins act as short-circuits to the capacitance between the radiating patch and the ground plane. In [31], it is approximated that the inductance due to the shorting pins is set in parallel with the antenna capacitance, creating an antiresonating circuit which explains the presence of a parallel resonance. TM_{00} which is below TM_{01} depends on the number of shorting pins and the size and the positions of them. Note that in the literature, the TM_{01} mode occurs a factor of 2.5 above the TM_{00} mode in frequency domain. Herein, by introducing more shorting pins, the number of physical parameters are increased which allow easier control of both TM_{00} and TM_{01} modes. Therefore, both modes are made use of within the operating band.

The resonance frequency at any TM_{mn} mode can be calculated by Eqn 1 [33] for an undisturbed rectangular patch where m and n are the mode numbers, pw is the width, pl is the length and L_e is the effective length of the patch, h is the thickness of the substrate. The effective dielectric constant, ϵ_e, is less than the relative dielectric constant, ϵ_r, due to the fact that the fields are not confined only in the dielectric medium and but also in the air and it can be calculated using Eqn 2. Taking the fringing capacitance account by inserting Eqn 3 into $L_e = pl + 2\Delta L$, the first three resonances are calculated to be the TM_{01}, TM_{02} and TM_{03} at 1.557 GHz, 3.114 GHz and 4.671 GHz. Eigenmode analysis conducted in Ansys Electronic Desktop [34] shows that these modes occur at 1.388 GHz, 2.776 GHz and 4.165 GHz. Once the shorting pins are introduced, TM_{01} is shifted higher in frequency to 2.49 GHz, as well as the TM_{00} mode being excited at 2.47 GHz.

Fig. 3 Diagram of the proposed antenna and the optimized parameters: slot length (*sl*), slot width (*sw*), patch length (*pl*), patch width (*pw*), transverse pin position (*tpp*), longitudinal pin positions (*lpp*), feed position (*fp*).

$$f_{mn} = \frac{c}{2\sqrt{\epsilon_e}} \sqrt{\left(\frac{m}{pw}\right)^2 + \left(\frac{n}{L_e}\right)^2} \qquad Eqn\ 1$$

$$\epsilon_e = \frac{\epsilon_r + 1}{2} + \frac{\epsilon_r - 1}{2}\left(1 + \frac{10h}{pw}\right)^{-1/2} \qquad Eqn\ 2$$

$$\Delta L = 0.412h \frac{(\epsilon_e + 0.3)\left(\frac{pw}{h} + 0.264\right)}{(\epsilon_e - 0.258)\left(\frac{pw}{h} + 0.8\right)} \qquad Eqn\ 3$$

As a guideline, the patch size can be chosen as $0.7\lambda_{guided}$ by $0.2\lambda_{guided}$, where λ_{guided} is the wavelength of the guided signal. Then the structure can be tuned using several parameters such as patch size (*pl* and *pw*), positions of the pins (*lpp* and *tpp*) and the feed position (*fp*) as labelled in Fig. 3. The frequency of both modes is controlled by the overall perimeter (*pw+pl*)

as well as the longitudinal pins. As *tpp* increases, the resonant frequency of the azimuth mode increases incrementally. An increase in *fp* results in a shift towards a lower frequency for the elevation mode. Therefore, *tpp* together with *fp* can be increased to shift the modes towards each other in frequency domain.

The proposed antenna as seen in Fig. 4 is excited with a coaxial feed. And prototyped on Rogers RT/duroid 6006 with relative permittivity, ϵ_r, of 6.15 and loss tangent, *tanδ,* of 0.0019. The overall dimensions of the antenna are 45 mm x 14 mm x 2.5 mm. The patch length (*pl*) is 41.5 and the patch width (*pw*) is 9 mm. Radii of the shorting pins are 0.8 mm. The offset of the feed from the center (*fp*) is 7.75 mm. The offset of the longitudinal pins (*lpp*) and the transverse pins (*tpp*) are 10.5 mm and 3.6 mm respectively. The TM_{00} mode of the antenna generates a main beam directed towards $\varphi=0°$, $\theta=62°$ [35]. In this paper, this mode is referred to as the azimuth mode. The TM_{01} mode, which has a main beam directed towards $\varphi=0°$, $\theta=12°$ is referred to as the elevation mode from this point forward.

C. Results

The simulated and measured frequency responses of the optimized antenna are compared in Fig. 5. A good agreement has been observed between the predictions and the measurements. However, the matching of the elevation mode was overestimated. The reason is believed to be the imperfections in the prototyping process.

The performance of an antenna is affected by its surroundings; therefore, an on-body antenna should be analysed with this fact in mind specifically because it is going to operate near the lossy human body at all times.
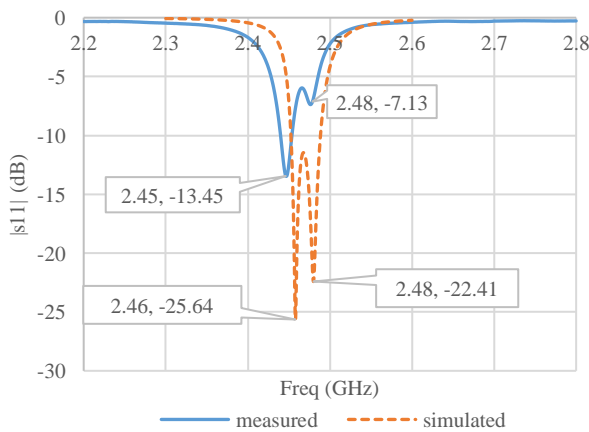

Fig. 5 The measured frequency response of the antenna compared to Ansys Electronics Desktop simulations
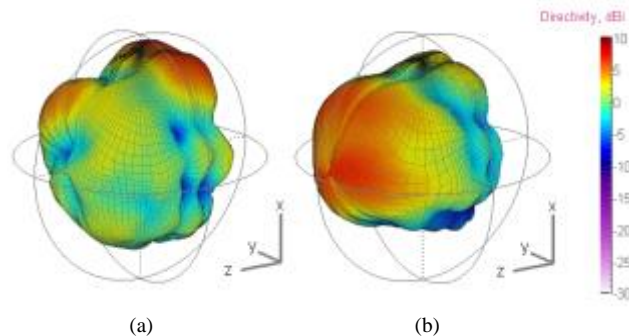

(a)   (b)

Fig. 6 3D Directivity (dBi) plots of (a) the azimuth mode and (b) the elevation mode

Fig. 6 shows the azimuth mode pattern in the beginning of the band and the elevation mode at the end of the band. These patterns have been measured in an anechoic chamber with the antenna mounted on a body phantom [36]. It can be seen that the former results in a null in the +z direction and the max radiation is in the x-y plane, whereas the latter directs all the energy to the +z direction. Maximum directivities observed for the azimuth mode and the elevation mode are 6.5 dBi and 6.6 dBi respectively. Ripples can be noticed which are due to the effect of the body. The experiments that follow evaluate the benefits of this pattern switching in a multipath environment through ray-tracing simulations and real-world measurements in a residential environment. The performance of the antenna is demonstrated in Section IV and V.

IV. SIMULATED ANTENNA PERFORMANCE EVALUATION

The ray-tracing study was performed in the virtual three-storey test house shown in Fig. 2. The performance of the proposed antenna was compared to that of the single mode directional patch and a single mode omnidirectional monopole to quantify the benefits of the switching radiation mode technique. Results from ray-tracing were combined with the radiation models from chamber measurements to simulate the channel.

Initially, a ray-tracing algorithm predicted all the direct, reflected and diffracted rays at 2.44 GHz for two scenarios: the AP and the user are located in the same room (AP 1 – Client 1 in Fig. 2); the access-point and the user are located in adjacent rooms (AP 1 – Client 2 in Fig. 2). In both cases, the user was rotated through 360º in azimuth, and the measured 3D polarimetric radiation patterns for a wrist-mounted omnidirectional and directional patch antenna were spatially convolved with the predicted multipath components. It should be noted that both elements have a similar measured radiation efficiency with that of the proposed antenna. The measured pattern of a vertical dipole was used at the side of the AP. Fig. 7 shows the received power at the user as a function of the body rotation for the two different antenna types in the two scenarios. When the user faces towards the direction of the dominant propagation path, the received signal strength is stronger by up to approximately 8 dB with the directional antenna, whereas as the user turns towards other directions the omnidirectional antenna provides more stable performance, better by up to about 8 dB than the directional one.
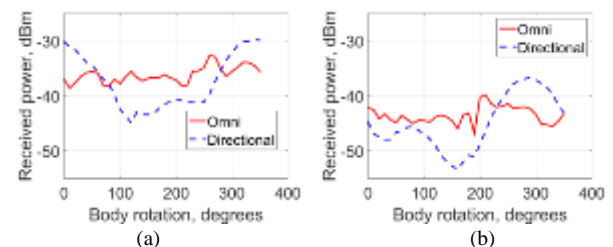

(a)   (b)

Fig. 7 Received power at the user as a function of body rotation.(a) access-point and user in same room; (b) access-point and user in adjacent rooms.

To obtain further insight into the received signal strength advantages of frequency dependent pattern switching, the ray-tracing simulation was used to analyse antenna performance in different topologies in the test house. Fig. 8 shows the improvement in received signal strength for different topologies achieved by switching between radiation

modes when advantageous. Improvement is relative to the best single radiation mode on average for that topology. There is always an advantage to being able to switch between patterns regardless of topology with a maximum improvement of 2.9 dB. Greatest gains are achieved when the AP is nearer to the UE, with both separation by walls on the same floor, and separation by multiple floors decreasing the advantages of pattern switching. In the situation where AP and user are separated by two floors, the improvement in received signal strength due to pattern switching is only 1.4 dB.
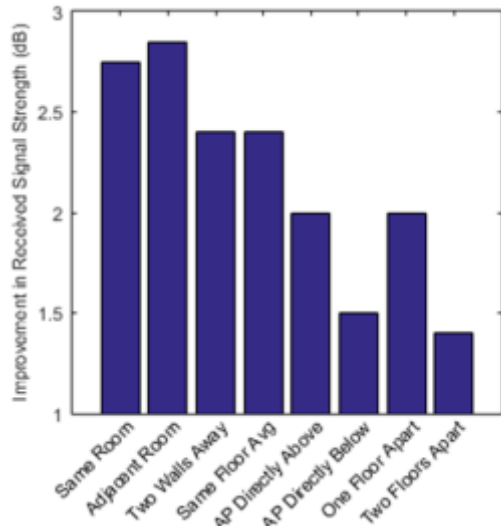

Fig. 8 Improvement in received signal strength due to frequency dependent pattern diversity relative to the best single radiation mode in a variety of user-AP topologies. Pattern switching is advantageous regardless of topology.

A total of nine antenna positions were used for ray-tracing simulations. These were generated by having the arm straight down by the side of the body (positions 1,4,7), a 45° bend at the elbow (positions 2,5,8) and a 90° bend at the elbow (positions 3,6,9). At each of these arm positions the antenna was mounted on the thumb side of the wrist, and the wrist was rotated clockwise 0° (positions 7,8,9), 90° (positions 4,5,6) or 180° (positions 1,2,3). Fig. 9 shows these positions.

Fig. 10 shows the difference in received signal strength between best and worst radiation mode. It should be noted there is no switching, the best radiation pattern on average relative to the worst is shown. Fig. 10 shows all antenna positions either with the AP on the same floor as the user or with the AP upstairs with respect to the user. In Fig. 10 if a bar is below zero on the dB scale it represents the directional pattern being better, in terms of received signal strength, than the omnidirectional pattern, and if above it represents the omnidirectional pattern's improvement over the directional pattern. Taking the example situation where the AP is upstairs relative to the user if the antenna is in position 2, an omnidirectional radiation pattern results in an extra 5.9 dB of signal strength compared to the directional pattern. If a user were to move their arm such that the antenna was in position 9, now the directional pattern achieves a 4.7 dB improvement in received signal strength over the omnidirectional. Another example is if the antenna is in position 4 on the same floor as the AP there is a 7.3 dB advantage to using the directional pattern, however if the user were to move downstairs relative to the AP with the same antenna position, 4, there is a 3.3 dB improvement from using the omnidirectional pattern. It can

be observed that both arm position and topology significantly affects which radiation pattern is optimal. This motivates the use of the proposed antenna, which may switch between radiation modes in a normal domestic case in which users are mobile.
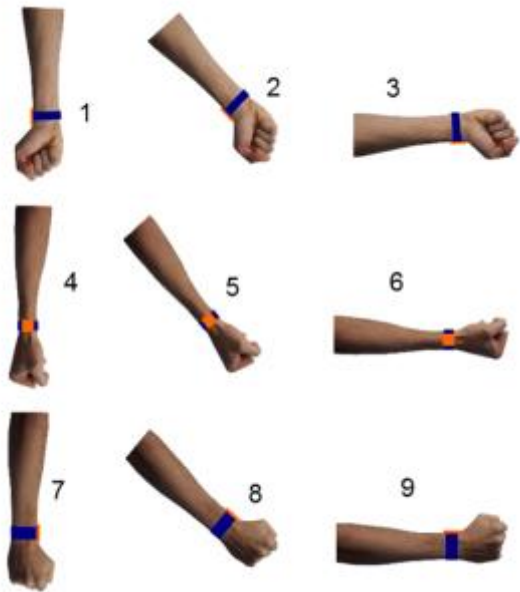

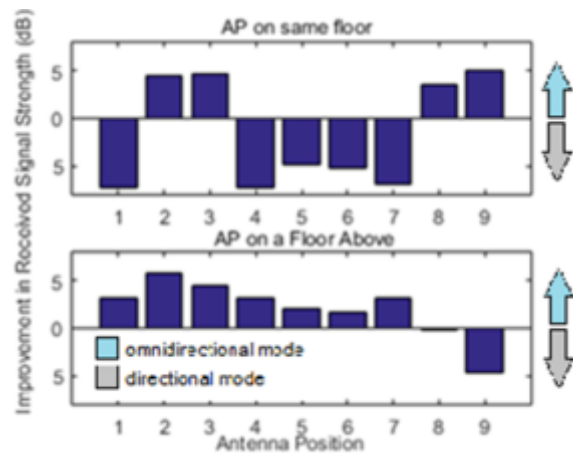Fig. 9 Antenna positions. Orange patch represents antenna position.

Fig. 10 Difference in received signal strength due to choosing the radiation mode that gives the best performance on average for various antenna positions. Two topologies are shown. The figure demonstrates that an antenna design that could switch between radiation modes is desirable since different arm positions and topology cause optimal radiation mode to change.

To simulate the proposed antenna design, an investigation was carried out to demonstrate the advantage of switching compared to picking a single radiation mode. By choosing the best radiation mode in a given situation the pattern switching antenna could be simulated. Fig. 11 shows how, in all elbow positions, pattern diversity facilitates an improved received signal strength versus both the worst and best case single pattern mode. In our case, this shows not only that there is an advantage to choosing a single best radiation mode, but that there is further significant advantage to switching between modes as and when this maximizes received signal strength. A minimum improvement of 1.6 dB can be observed in Fig. 11 which is relative to a well-chosen single pattern antenna for a zero-degree elbow bend. A maximum of improvement of 4.3 dB is achieved compared to a poorly chosen single radiation pattern in the same elbow orientation.
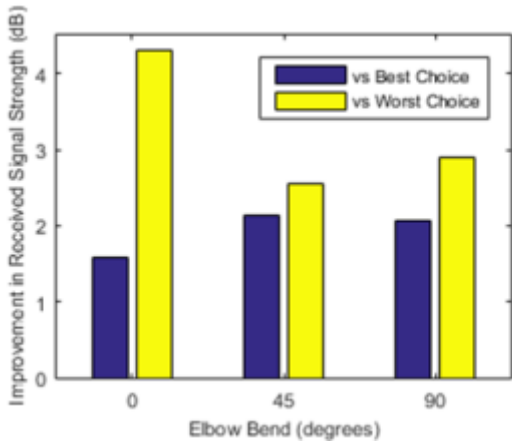
Fig. 11 Improvement in received signal strength due to switching between radiation modes when advantageous relative to the best and worst single radiation modes for three elbow positions. This illustrates that the use of pattern diversity always results in an improved received signal strength when compared to an antenna with a single radiation mode.
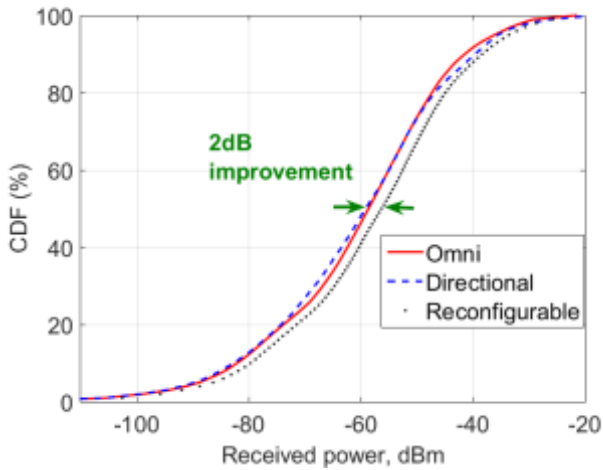

Fig. 12 CDF of received power for the three different user antennas over the 94,500 links in the virtual test-house.

Finally, taking all the simulations into account, the performance of the omnidirectional, the directional and the reconfigurable antenna proposed in this paper is compared for ten access-point and ten user locations randomly distributed in all the rooms around the test-house, as shown in Fig. 2. In all cases, the user was rotated through 360° in steps of 10° and nine different wrist positions were considered. All analysis was repeated for three orthogonal dipoles at the access-point, resulting in a total of 94,500 links for each user antenna. This number of links would be impractical to measure in the real world. Fig. 12 shows the Cumulative Distribution Function (CDF) of the received power for the three user antennas under test. When such a large number of links is investigated, differences tend to average out and hence and we can see that the CDF graphs for the omnidirectional and for the directional antennas are almost identical. The proposed antenna, however, shows a significant median improvement of approximately 2 dB due to frequency dependent pattern switching. This is a useful result for the system designer. The simulations have demonstrated the advantages of the example antenna. If results had shown poor performance compared to a single radiation mode the antenna designer could redesign the antenna until the specified performance was achieved. We also gain useful insights into antenna performance in different situations. For example, omnidirectional antennas tend to

give superior performance when communication takes place between floors, to a maximum of a 5dB improvement, whereas directional antennas give better performance on the same floor unless the arm position is such that the main lobe is directed towards the floors above or below.

V. VERIFICATION AGAINST MEASUREMENTS

In this section, we experimentally evaluate the performance of the proposed antenna in a real residential environment, namely the SPHERE (a Sensor Platform for Healthcare in a Residential Environment) house [37], for an off-body scenario in which the on-body node communicates with a nearby access-point. Measurements here represent a final verification step, demonstrating that results generated in simulations are realistic.

The SPHERE house is a fully furnished two-storey house with brick walls located in the city-centre of Bristol, UK. Fig. 13 shows the floor plan of the SPHERE house including the access-point (AP1-AP4) and the wearable (W1-W3) measurement locations. Measurements included the wireless channel gain and the system-level performance of a real BLE system.

The off-body wireless channel gain (which includes not only path loss but also the transmit and receive antenna gains) was measured in the 2.4 GHz band using a Vector Network Analyser (VNA) following a measurement procedure similar to that described in [37]. The measurements were performed with the proposed antenna mounted on the wrist of a human subject (male, 176 cm height, 80 kg weight) in locations W1, W2 and W3 for two different arm positions and with the subject rotating through 360º in azimuth. The investigated links are classified into the following five categories: Same room (AP1-W1, AP2-W1, AP3-W2); one wall (AP1-W2, AP2-W2, AP3-W1, AP3-W3); two walls (AP1-W3, AP2-W3); and first-to-ground floor (AP4-W1, AP4-W2, AP4-W3).

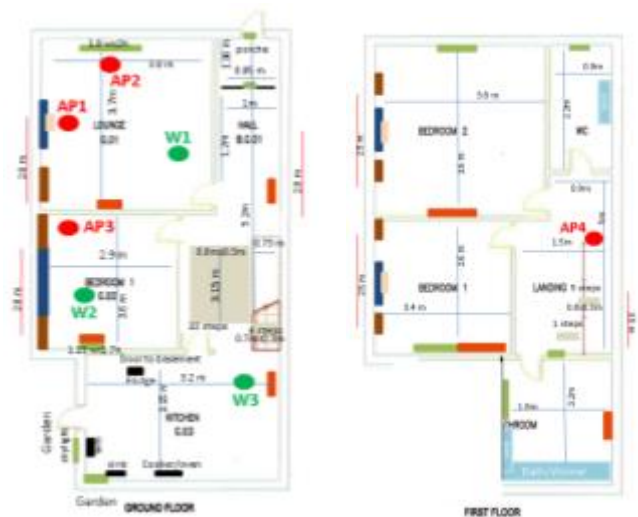Fig. 13 Floor-plan of the SPHERE house showing the access-point (AP1-AP4) and the wearable (W1-W3) measurements locations.

Fig. 14 shows the CDFs of the measured mean channel gain for the four link categories. Fig. 14 refers to the case of the AP employing a horizontal dipole antenna. Results are similar for a vertical dipole. Each CDF graph is calculated over all the body azimuth rotations and the two arm positions.

The mean (μ) and the standard deviation (σ) for each CDF graph are also indicated in Fig. 14. We can observe that each (concrete) wall introduces an extra loss of 19 dB in average when the access-point and the user are on the same floor level. Note that this value includes the additional path loss due to longer distance separations between the transmitter and the receiver and does not refer to losses due to the wall only. Furthermore, the standard deviation of each CDF graph demonstrates the effect of body shadowing. This was found to be about 6 dB for the same-room links, 5.9 dB for the one-wall links, 4.1 dB for the two-wall links, and 4.7 dB for the first-to-ground floor links. We can notice that the effect of the body is stronger in the same-room and in the one-wall links, where a strong propagation path dominates the wireless link.

Fig. 14 also demonstrates the Packet-Error-Rate (PER) as a function of the wireless channel gain that was measured for a BLE system that uses the Nordic nRF51822 chipset in connectionless mode (broadcasting in the three advertising channels) [37]. Assuming a transmit power of 0 dBm, which is common for such systems, the received signal power will be equal to the channel gain. If we hence assume a PER of 1% as an acceptable outage threshold, a single AP in the SPHERE house could sufficiently cover all the cases in the same room, in adjacent rooms on the same floor level, and in upstairs-to-downstairs communication, and only 40% of the cases when the transmitter and the receiver are separated by two walls. This indicates the need of multiple AP deployment for full wireless coverage in the SPHERE house if a BLE system is employed.
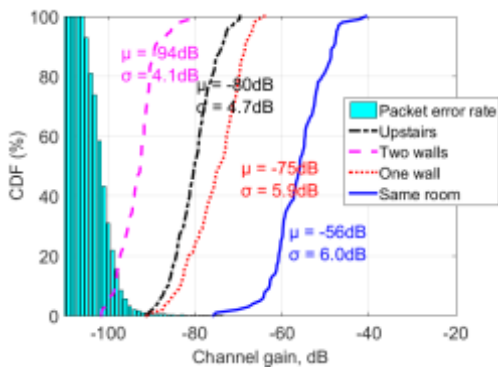

Fig. 14 CDF (over the two arm positions and all body rotations) of channel gain in the four link categories using a horizontal dipole at the access-point Mean (μ) and standard deviation (σ) are indicated. The PER for a BLE system is also shown (assuming a 0 dBm transmit power the channel gain is equal to received signal power).
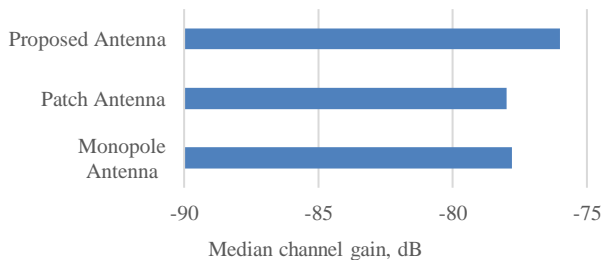

Fig. 15 Median channel gain over all the measurements.

For comparison and benchmarking purposes, all wireless channel measurements were repeated with two additional wearable antennas, namely a custom patch antenna [37] and an off-the-shelf monopole antenna (nRF51822-EK). The former has a directional and the latter an omnidirectional radiation pattern over the whole 2.4 GHz frequency band. Fig. 15 shows the measured median channel gain for the three candidates, which was found to be approximately 2 dB better for our proposed antenna, a result that agrees with the conclusions from the ray-tracing simulations of Section III. This 2 dB improvement in performance highlights the fact that the benefit of frequency dependent radiation pattern switching can be quite significant, especially if we consider the fact that it was calculated over all the links in the SPHERE house, access-point antennas, arm positions, and body orientations. The agreement with ray-tracing demonstrates how the proposed method is a valid means quantifying antenna performance.

Finally, a series of free-walking experiments were conducted in order to identify the behaviour of the proposed antenna in dynamic scenarios. The user with the wrist-mounted antenna is randomly walking inside the lounge (same room as AP1 in Fig. 13) for 20 minutes, covering all the available area within the room, and three AP locations were considered: AP1 (i.e. user and AP are in the same room), AP3 (one wall separation between the user and the AP) and AP4 (upstairs-to-downstairs link). Fig. 16 shows the CDF of the channel gain for each of these three-dynamic links and the results demonstrate similar behaviour to the static measurements shown in Fig. 14.
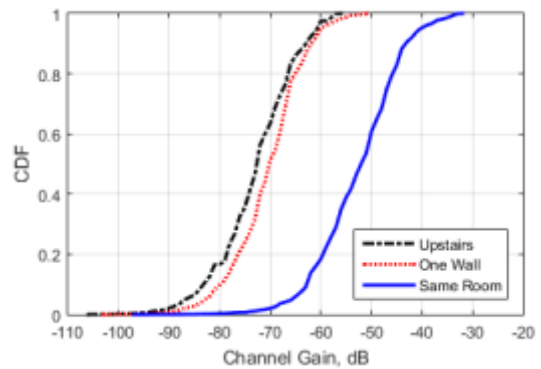

Fig. 16 CDF of the channel gain in three dynamic links, where the user with the wrist-mounted antenna performs random walks within a room.

VI. CONCLUSIONS

A method for quantifying the performance of an antenna design was presented. As a case study, a planar antenna capable of radiation pattern switching by changing the maximum radiation direction with frequency was presented. At the lower end of the frequency band up to 2.45 GHz, the antenna generates nulls away from the antenna's main axis. On the other hand, for the rest of the band, a directional radiation pattern away from the antenna's main axis is formed.

The performance of the proposed antenna was analysed using the proposed method which included extensive ray-tracing simulations in conjunction with antenna pattern measurements including the effects of the body. A detailed investigation was performed to practically demonstrate the sensitivity of the link quality on the antenna position on the wrist and on the arm orientation. It was shown, that the frequency dependent pattern switching technique may result in large benefits, as high as 8 dB for specific links. The analysis of the antenna showed, in this test case, that the example antenna achieved good performance but could also be used to identify poor antenna designs or compare candidate antennas in specific situations.

Then the performance of the antenna was investigated in a real off-body propagation scenario in a residential environment. The proposed antenna was mounted on the wrist of a human subject and communicated with a nearby access-point. The impact of body-shadowing was quantified, showing that the standard deviation of the received signal due to body rotation is approximately 6 dB in links where a strong signal path is present, and about 4 dB in links where weaker multipaths are the main propagation mechanism. Furthermore, the benefit of pattern switching was highlighted as the median performance of the proposed antenna was found to be 2 dB better than that of a patch antenna with directional pattern only, and that of a monopole antenna with omnidirectional pattern only over the whole band. This result was calculated over all the measured links in the house, access-point antennas, arm positions, and body orientations and was in agreement with the conclusions from the ray-tracing simulations; demonstrating how the ray-tracing simulations can be used to effectively quantify antenna performance in the design phase of an off-body communication system.

REFERENCES

[1] N. Zhu, T. Diethe, M. Camplani, L. Tao, A. Burrows, N. Twomey, D. Kaleshi, M. Mirmehdi, P. Flach, and I. Craddock, "Bridging e-Health and the Internet of Things: The SPHERE Project," *IEEE Intell. Syst.*, vol. 30, no. 4, pp. 39–46, Jul. 2015.

[2] M. Chan, D. Estève, J.-Y. Fourniols, C. Escriba, and E. Campo, "Smart wearable systems: current status and future challenges," *Artif. Intell. Med.*, vol. 56, no. 3, pp. 137–56, Nov. 2012.

[3] L. Atzori, A. Iera, and G. Morabito, "The Internet of Things: A survey," *Comput. Networks*, vol. 54, no. 15, pp. 2787–2805, Oct. 2010.

[4] S. Ullah, H. Higgins, B. Braem, B. Latre, C. Blondia, I. Moerman, S. Saleem , Z. Rahman, and K. Sup Kwak, "A Comprehensive Survey of Wireless Body Area Networks," *J. of Medical Systems*, vol. 36, no. 3, pp. 1065-1094, Aug. 2010.

[5] A. R. Chandran, G. A. Conway, W. G. Scanlon, "Pattern switching compact patch antenna for on-body and off-body communications at 2.45 GHz," *EuCAP 2009. 3rd European Conference on Antennas and Propagation,* vol., no., pp.2055-2057, 23-27 March 2009.

[6] P.S. Hall, Y. Hao, Y. I. Nechayev, A. Alomainy, C. C. Constantinou, C. Parini, M. R. Kamarudin, T. Z. Salim, D. T. M. Hee, R. Dubrovka, A. S. Owadally, S. Wei, A. Serra, P. Nepa, M. Gallo, M. Bozzetti, "Antennas and propagation for on-body communication systems," *IEEE Antennas and Propagation Magazine*, vol.49, no.3, pp.41,58, June 2007.

[7] Z. Lanlin, W. Zheyu, J.L. Volakis, "Textile Antennas and Sensors for Body-Worn Applications," I*EEE Antennas and Wireless Propagation Letters*, vol.11, no., pp. 1690-1693, 2012.

[8] Z. G. Liu and Y. X. Guo, "Dual band low profile antenna for body-centric communications," *IEEE Trans. Antennas. Propag.*, vol. 61, no. 4, pp. 2282–2285, Apr. 2013.

[9] K. Seonghun, W. J. Chang, "Wearable fabric antenna on upper arm for MedRadio band applications with reconfigurable beam capability*," in Electronics Letters*, vol.51, no.17, pp.1314-1316, 2015.

[10] T. B. Welch, R. L. Musselman, B. A. Emessiene, P. D. Gift, D. K. Choudhury, D. N. Cassadine, and S. M. Yano, "The Effects of the Human Body on UWB Signal Propagation in an Indoor Environment," *IEEE Journal on Selected Areas in Communications*, no. 9, pp. 778–1782, 2002.

[11] Q. H. Abbasi, M. M. Khan, S. Liaqat, A. Alomainy, and Y. Hao, "Ultra Wideband Off-body Radio Channel Characterisation for Different Environments," *7th International Conference on Electrical Computer Engineering (ICECE)*, pp. 165–168, 2012.

[12] A. A. Goulianos, T. W. C. Brown, B. G. Evans, and S. Stavrou. "Wideband Power Modeling and Time Dispersion Analysis for UWB Indoor Off-Body Communications*." IEEE Transactions on Antennas and Propagation,* vol. 57, no. 7, pp. 2162–2171, 2009.

[13] M. M. Khan, Q. H. Abbasi, A. Alomainy, Y. Hao and C. Parini, "Experimental characterisation of ultra-wideband off-body radio channels considering antenna effects," *in IET Microwaves, Antennas & Propagation*, vol. 7, no. 5, pp. 370-380, April 2013.

[14] S. L. Cotton, and W.G. Scanlon, "Characterization and Modeling of the Indoor Radio Channel at 868 MHz for a Mobile Bodyworn Wireless Personal Area Network," *IEEE Antennas and Wireless Propagation Letters,* vol. 6, pp. 51–55, 2007.

[15] S. L. Cotton, and W. G. Scanlon, "Indoor Channel Characterisation for a Wearable Antenna Array at 868 MHz," *IEEE Wireless Communications and Networking Conference*, WCNC 2006, pp. 1783–1788, 2006.

[16] R. Rosini, and R. D'Errico, "Off-Body Channel Modelling at 2.45 GHz for Two Different Antennas," *6th European Conference on Antennas and Propagation (EUCAP),* pp. 3378–3382, 2012.

[17] R. Rosini, and R. D'Errico, "Space-time Correlation for on-to-Off Body Channels at 2.45 GHz," *7th European Conference on Antennas and Propagation (EuCAP),* pp. 3529–3533, 2013.

[18] D. S. Yang, "A New Radio Propagation Model at 2.4 GHz for Wireless Medical Body Sensors in Outdoor Environment," *35th Annual International Conference of the IEEE Engineering in Medicine and Biology Society (EMBC),* pp. 3269–3273, 2013.

[19] D. B. Smith, D. Miniutti, and L. W. Hanlen, "Characterization of the Body-Area Propagation Channel for Monitoring a Subject Sleeping," *IEEE Transactions on Antennas and Propagation*, vol. 59, no. 11, pp. 4388–4392, 2011.

[20] T. Kikuzuki, A. S. Andrenko, M. G. S. Hossain, I. Ida, K. Kasai, and Y. Ohashi, "A Simple Path Loss Model for Body Area Network in the Bed Side Monitoring Applications," *Microwave Conference Proceedings (APMC), 2011 Asia-Pacific*, pp. 765–768, 2011.

[21] R. D. Francisco, "Indoor Channel Measurements and Models at 2.4 GHz in a Hospital," *IEEE Global Telecommunications Conference (GLOBECOM 2010)*, pp. 1–6, 2010.

[22] S. H. Kvist, P. F. Medina, J. Thaysen, and K. B. Jakobsen. "On-body and Off-body 2.45 GHz MIMO Communications for Hearing Instrument Applications," *7th European Conference on Antennas and Propagation (EuCAP)*, pp. 2595–2599, 2013.

[23] D. Miniutti, L. Hanlen, D. Smith, A. Zhang, D. Lewis, D. Rodda, B. Gilbert, "Narrowband on body to off body channel characterization for ban," *IEEE 802.15-08-0559-00-0006*, August 2008.

[24] B.S. Lee, A.R. Nix, and J.P. McGeehan, "Site specific prediction and measurement of indoor power delay and power azimuth spectra at 5 GHz," *54th IEEE Vehicular Technologies Conference (VTC-Fall),* vol. 1, pp. 733-737, 2001.

[25] B.S. Lee, A.R. Nix, and J.P. McGeehan, "A spatio-temporal ray launching propagation model for UMTS pico and microcellular environments," *53rd IEEE Vehicular Technologies Conference (VTC-Spring),* vol. 1, pp. 367-371, 2001.

[26] B.S. Lee, A.R. Nix, and J.P. McGeehan, "Indoor space-time propagation modelling using a ray launching technique," *11th International Conference on Antennas and Propagation*, vol. 1, pp. 279 -283, 2001.

[27] S. Dumanli, "A radiation pattern diversity antenna operating at the 2.4 GHz ISM band," IEEE *Radio and Wireless Symposium (RWS), 2015*, pp. 102-104, Jan 2015.

[28] T. Kikuzuki, A. S. Andrenko, M. G. S. Hossain, I. Ida, K. Kasai, Y. Ohashi, "A simple path loss model for body area network in the bed side monitoring applications," *Asia-Pacific Microwave Conference Proceedings (APMC)*, pp. 765 - 768, Dec. 2011.

[29] V. Gonzalez-Posadas, D. Segovia-Vargas, E. Rajo-Iglesias, J. L. Vazquez-Roy, C. Martin-Pascual, "Approximate analysis of short circuited ring patch antenna working at TM01 mode*," IEEE Transactions on Antennas and Propagation,* vol.54, no.6, pp. 1875 - 1879, June 2006.

[30] N. Merce, P. Tejedor, J. Vassal'lo, "The TM01 mode of microstrip radiators and some of its applications," *Ninth International Conference on Antennas and Propagation, (Conf. Publ. No. 407)*, pp. 33 - 36 vol.1, 4-7 Apr 1995.

[31] C. Delaveaud, P. Leveque, and B. Jecko, "New kind of microstrip antenna: The monopolar wire-patch antenna," *IEEE Electron. Letters*, vol. 30, no. 1, pp. 1–2, Jan. 1994.

[32] G. A. Conway, W. G. Scanlon, "Antennas for over-body-surface communication at 2.45 GHz", *IEEE Transactions on Antennas and Propagation*, vol. 57, no. 4, pp. 844 - 855, April 2009.

[33] K. Girish, and K. P. Ray. *Broadband microstrip antennas.* Artech House, 2002.

[34] [Online], Available: http://www.ansys.com/Products/Simulation+Technology/Electronics/Signal+Integrity/ANSYS+HFSS, accessed February 2017.

[35] S. Dumanli, "On-body antenna with reconfigurable radiation pattern," *IEEE MTT-S International Microwave Workshop Series on RF and Wireless Technologies for Biomedical and Healthcare Applications (IMWS-Bio),* pp.1-3, Dec. 2014.

[36] H. Giddens, D. L. Paul, G. S. Hilton and J. P. McGeehan, "Numerical and experimental evaluation of phantoms for off-body wireless communications," 2011 Loughborough Antennas & Propagation Conference, Loughborough, 2011.
[37] X. Fafoutis, E. Tsimbalo, E. Mellios, G. Hilton, R. Piechocki, and I. Craddock, "A residential maintenance-free long-term activity monitoring system for healthcare applications," *EURASIP J. Wirel. Commun. Netw.*, vol. 2016, no. 1, p. 31, Jan. 2016.

Sema Dumanli received the BSc degree in electrical and electronic engineering from Orta Dogu Teknik Universitesi (ODTU), Ankara Turkey in 2006 and the PhD degree from University of Bristol, Bristol, UK, in 2010.

She had worked in Toshiba Research Europe, Bristol UK as a research engineer and a senior research engineer from August 2010 to January 2017. She is currently an Assistant Professor at Bogazici University, Istanbul Turkey and a consultant in Republic of Turkey Ministry of Health. Her current research interests include antenna design for body area networks, implantable and wearable devices, eHealth and MIMO communications.

Lawrence Sayer was born in Portsmouth, UK, in 1992. He received an MEng degree in electronic and communications engineering from the University of Bristol, UK, in 2014. He is currently studying for a PhD at the EPSRC Centre for Doctoral Training in Communications at the University of Bristol. His research interests include: propagation modelling, millimetre wavelength communications and security of 5G networks.

Evangelos Mellios is a Lecturer in Electrical & Electronic Engineering at the University of Bristol. He took up his post in 2015 having previously completed his PhD in Bristol's Communication Systems & Networks Group in the field of antennas and wireless propagation. Evangelos also holds a Diploma in Electrical & Computer Engineering from the Aristotle University of Thessaloniki, and an MSc degree in Communication Systems & Signal Processing from the University of Bristol. His research interests lie in the field of antennas, wireless propagation and PHY-layer system-level measurements, analysis, modelling and design for a variety of wireless technologies and applications. These include 5G cellular networks (with a focus on millimeter-wave and sub-6GHz Massive MIMO enabling technologies), Wi-Fi communication systems, and low power body-centric and Internet-of-Things applications.

Xenofon Fafoutis (S'09-M'14) received a PhD in Embedded Systems Engineering from the Technical University of Denmark in 2014; an MSc degree in Computer Science from the University of Crete in 2010; and a BSc in Informatics and Telecommunications from the University of Athens in 2007.

He was also associated with the Foundation for Research and Technology - Hellas (FORTH). Since 2014, he is a researcher with the University of Bristol and a member of the EPSRC SPHERE interdisciplinary research collaboration. His interests lie in the fields of wireless embedded systems, wireless sensor networks and the internet of things.

Geoffrey S. Hilton received the B.Sc. degree from the University of Leeds, Leeds, U.K., in 1984. He received the Ph.D. degree from the University of Bristol, Bristol, U.K., in 1993 for research into the design and Finite-Difference Time-Domain modelling of printed antenna elements. He was a Design Engineer with GEC-Marconi before his involvement with Bristol University, where he is currently a Senior Lecturer. His research interests include practical antenna and system design for a variety of communications and radar applications such as Ground Penetrating Radar, performance evaluation of antennas in mobile radio, electrically small elements, active/tuneable elements and vehicle-mounted conformal antennas.

Ian J. Craddock (M'09-SM'10-F'16) is currently a full Professor with the University of Bristol (UK) and Director of the flagship "SPHERE" centre (www.irc-sphere.ac.uk) comprising approximately 100 researchers and clinicians working on IoT technology for health. He has been working in healthcare technology for 15 years and founded a company that is currently completing trials of a CE-marked breast imaging device based on his research. He has published over 150 papers and serves on the healthcare strategy board for the UK's largest engineering funder. He is also separately employed by Toshiba as Managing Director of their Telecommunications Research Lab in Bristol, responsible for a portfolio of both internal and collaborative communications, IoT and smart city research.